ACS APPLIED MATERIALS & INTERFACES

Research Article

www.acsami.org

Engineering Adhesion to Thermoresponsive Substrates: Effect of Polymer Composition on Liquid–Liquid–Solid Wetting

Filippo Gambinossi,[†] Lauren S. Sefcik,[†] Erik Wischerhoff,[‡] Andre Laschewsky,[‡,§] and James K. Ferri*[,†]

[†]Department of Chemical and Biomolecular Engineering, Lafayette College, 740 High Street, Easton18042, Pennsylvania, United States

[‡]Fraunhofer Institute for Applied Polymer Research, Geiselbergstrasse 69, D-14476 Potsdam-Golm, Germany

[§]Institute of Chemistry, University of Potsdam, Karl-Liebknecht-Str. 24-25, D-14476 Potsdam-Golm, Germany

Supporting Information

ABSTRACT: Adhesion control in liquid–liquid–solid systems represents a challenge for applications ranging from self-cleaning to biocompatibility of engineered materials. By using responsive polymer chemistry and molecular self-assembly, adhesion at solid/liquid interfaces can be achieved and modulated by external stimuli. Here, we utilize thermosensitive polymeric materials based on random copolymers of di(ethylene glycol) methyl ether methacrylate (x = MEO_2MA) and oligo(ethylene glycol) methyl ether methacrylate (y = OEGMA), that is, P(MEO_2MA_x-*co*-$OEGMA_y$), to investigate the role of hydrophobicity on the phenomenon of adhesion. The copolymer ratio (x/y) dictates macromolecular changes enabling control of the hydrophilic-to-lipophilic balance (HBL) of the polymer brushes through external triggers such as ionic strength and temperature. We discuss the HBL of the thermobrushes in terms of the surface energy of the substrate by measuring the contact angle at water–decane–P(MEO_2MA_x-*co*-$OEGMA_y$) brush contact line as a function of polymer composition and temperature. Solid supported polyelectrolyte layers grafted with P(MEO_2MA_x-*co*-$OEGMA_y$) display a transition in the wettability that is related to the lower critical solution temperature of the polymer brushes. Using experimental observation of the hydrophilic to hydrophobic transition by the contact angle, we extract the underlying energetics associated with liquid–liquid–solid adhesion as a function of the copolymer ratio. The change in cellular attachment on P(MEO_2MA_x-*co*-$OEGMA_y$) substrates of variable (x/y) composition demonstrates the subtle role of compositional tuning on the ability to control liquid–liquid–solid adhesion in biological applications.

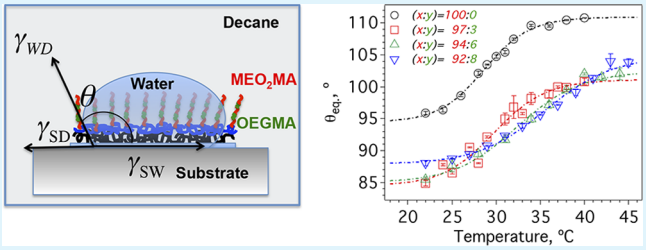

KEYWORDS: *water/decane contact angle, thermoresponsive substrates, di(ethylene glycol) methyl ether methacrylate, oligo(ethylene glycol) methyl ether methacrylate, hydrophilic-to-lipophilic balance, programmable adhesion*

1. INTRODUCTION

Surface wetting phenomena are ubiquitous and play an important role in several industrial processes as well as in daily life.[1] Wetting solutions have been proposed to solve technological problems such as oil recovery,[2] water collection,[3,4] and art conservation[5] and have helped to engineer biocompatible coatings,[6,7] self-cleaning systems,[8,9] and microfluidic devices.[10−12] In each circumstance, wetting phenomena are governed by the interplay of micro/nano structures and interfacial interactions acting along very small distances. Understanding the physical principles that rule wetting phenomena is therefore of crucial importance not only in understanding how and why a surface has been modified but also to design programmable systems. To this end, one of the major challenges is to engineer dynamic surfaces that change wetting and adhesion properties in real-time and enact such changes in response to external stimuli. Design and development of such structures require deep knowledge of both topology of the solid surface and the chemical properties of the fluid and solid phases. Recently, through the combination of substrate coating with stimuli-responsive materials and tailored surface patterning, reversible hydrophilic-to-hydrophobic switches have been realized.[13−15] Environmentally responsive polymers undergo sharp, reversible phase transitions in water as a result of a small change in pH, temperature, or ionic strength.[16] When grafted to a surface this results in a change in surface wettability.[17]

One of the most important aspects in biotechnological applications is the modification of surfaces to control cell behavior.[18,19] Removal of unwanted biofilms or biofouling requires interruption of the association between the cells and substrata and therefore also requires a better understanding of the substratum properties that are important in the maintainance of a biofilm. Release of mammalian cell sheets from tissue culture substrates is another example where substrate properties dictate the attachment/detachment

Received: October 25, 2014
Accepted: January 8, 2015
Published: January 8, 2015

DOI: 10.1021/am507418m
ACS Appl. Mater. Interfaces 2015, 7, 2518−2528

phenomena and influence cell behavior.[20,21] Hydrophobicity appears to play a role in maintaining cellular attachment in both cases. The ability of the temperature-responsive polymer poly(*N*-isopropylacrylamide) (PNIPAM) to reversibly attach and release both bacteria and mammalian cells has been demonstrated.[17,22] Above the lower critical solution temperature (LCST) of PNIPAM, cells attach to the relatively hydrophobic substrate and are released upon a temperature switch to below the LCST. This hydrophobic-to-hydrophilic phase transition has been shown to be reversible and is capable of maintaining cell−cell interactions during the release process. While PNIPAM substrates have shown promise in cell sheet engineering applications, concerns exist regarding toxicity of the monomer and decreased cell viability.[23] Different cell types have also shown differential responses to culture on PNIPAM. Hydrophobic copolymers of PNIPAM have been proposed to broaden their utiliy,[24] but it was found that the time required for cell detachment from these more hydrophobic copolymers led to slower release of cell sheets, thus deteriorating cellular metabolic functions at lower temperatures.[25] Using small percentages of *N*-*tert*-butylacrylamide (NTBAM) to increase surface hydrophobicity has been shown to enhance cell adhesion. However, this is attributed to the extra methyl group present in the NTBAM monomer compared to the PNIPAM monomer.[26] The effects of surface functional groups on cellular interactions and biocompatibility have been investigated, and it has been shown that hydroxyl groups (found on tissue culture polystyrene, TCP, for example) promote cellular adhesion and spreading compared to methyl groups.[27,28] Futhermore, methyl groups were found to increase the trafficking and adhesion of inflammatory cells in vivo, an undesirable side effect of biomaterial implantation.[29] Taken together, alternatives to PNIPAM have been explored, such as the 2-(2-methoxyethoxy)ethyl methacrylate (MEO_2MA)-based copolymers, for their structural similarity to poly(ethylene glycol), which is widely used in medical applications for its biocompatbility and nontoxicity. MEO_2MA copolymers also provide a hydroxyl side-chain functional group for chemical modifications, and the transition temperature can also be precisely tuned.[30]

The adhesive properties of PNIPAM, poly-*N*-[(2,2-dimethyl-1,3-dioxolane)methyl]acrylamide (PDMDOMA),[31] and polyethylene glycol-based[32−35] thermoresponsive polymer surfaces suitable to control cell adhesion[36] have been investigated using force measurements.[32] For all investigated polymers, adhesion was found to increase sharply above LCST and with increasing hydrophobicity of the atomic force microscopy (AFM) probe.[37] The effect of grafting density on adhesion forces was also investigated previously.[31,38] For instance, Kessel et al. (2010) studied the interaction forces between a native and a protein-coated probe and the thermoresponsive copolymer P(MEO_2MA_{90}-*co*-$OEGMA_{10}$) coated on gold surfaces using colloidal probe AFM.[32] Measurements were carried out in aqueous media (distilled water, phosphate-buffered saline (PBS) buffer, and cell culture media) at temperatures between T = 20 and 40 °C; a sharp transition in adhesion was observed in all cases below and above the LCST of the copolymer, which was T = 32 °C. The properties of the polymer-coated surfaces could be switched repeatedly without a loss of adhesive performance. Time-dependent measurements provided an insight into the kinetics of the switching process, showing that the maximum adhesion force was reached after 20 min upon heating and minimum adhesion approximately after 20 min after cooling. More recently, Synytska et al. (2010) compared the switchable adhesive performance of thermoresponsive polymer brushes with different architectures based on PNIPAM, poly(oligo(ethylene glycol) methyl ether methacrylate-*co*-2-(2-methoxyethoxy)ethyl methacrylate), P($OEGMA_{12}$-MEO_2MA_{88}), and poly(oligo(ethylene glycol) methyl ether methacrylate-*co*-oligo(propylene glycol) methacrylate), and P($OEGMA_{25}$-*co*-$OPGMA_{75}$) having an LCST ≈ 33 °C.[33,39] The adhesion measurements on flat and rough silicon substrates were performed in distilled water as a function of temperature, $24 < T$, °C < 40. It was concluded that the observed adhesion behavior depends on both the chemical structure of the brush and the surface geometry/roughness.[33,39] All brushes were found to be completely nonadhesive below the LCST, with strong attractive interactions observed on these systems at higher temperatures.

Understanding how and why this programmable adhesion process occurs requires systematic investigation over a range of water−oil−solid contact angles. Both surface morphology and chemistry are known to be key parameters in the control of wetting phenomena.[13,40−42] Although some authors have demonstrated the ability to manipulate the release behavior of a water droplet upon directional movement,[13,41] the effects of surface chemistry and nanoscale morphology on adhesion phenomena have only recently been explored.[43,44] One likely reason is that it is difficult to control both morphology and chemistry simultaneously to study the effects of adhesion to soft matter. Here, we explore a thermoresponsive polymeric system that undergoes a hydrophilic-to-hydrophobic phase transition at the LCST of the polymer.

In this work, we design thermoresponsive substrates based on random copolymers of 2-(2-methoxyethoxy)ethyl methacrylate (x = MEO_2MA) and oligo(ethylene glycol) methacrylate (y = OEGMA), P(MEO_2MA_x-*co*-$OEGMA_y$), to investigate the role of hydrophobicity on surface adhesion. These copolymers display LCST, which can be precisely adjusted by varying the comonomer composition[34] and directly dictates the contact angle and thus the adhesion properties. In particular, when grafted to nanoparticles (NPs), changes in ionic strength or temperature cause macromolecular conformational changes, leading to colloidal aggregation.[45−47] More recently, we studied the effect of surface hydrophobicity on NP equilibrium adsorption isotherms and compared fluid phase partitioning with cellular uptake. We observed an increase in cellular uptake for increasing (x/y) ratio suggesting that surface chemistry plays a key role in intercellular transport processes.[48]

Previously, we showed that P(MEO_2MA_{94}-*co*-$OEGMA_6$) substrates with an LCST of 34 °C supported mammalian cell attachment and spreading, with an observed time lag compared to gold-standard substrates UpCell (PNIPAM) and tissue culture polystyrene.[49] Here, we investigate using compositional effects to tune adhesion. P(MEO_2MA_x-*co*-$OEGMA_y$) substrates with LCSTs ranging between 28 and 37 °C are used to systematically study the effects of surface wettability via contact angle measurements on adhesion phenomena, independent of changes in surface chemistry or morphology. Initial attachment of fibroblast cells are used as an example to demonstrate that controlling the surface energetics by varying the (x/y) ratio in P(MEO_2MA_x-*co*-$OEGMA_y$) copolymers can have important implications in their success as programmable adhesive thermoresponsive surfaces.

DOI: 10.1021/am507418m
ACS Appl. Mater. Interfaces 2015, 7, 2518−2528

Scheme 1. Measurement of the Water Contact Angle in Decane and Schematic of P(MEO_2MA_x-*co*-$OEGMA_y$) Brushes Grafted on LbL Structure.

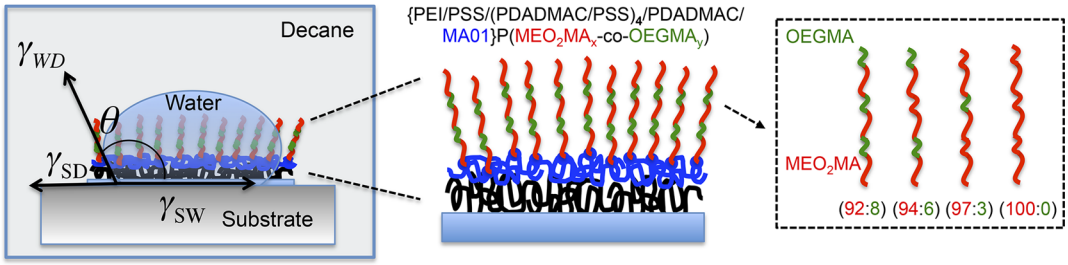

2. EXPERIMENTAL SECTION

2.1. Materials. Polyethylenimine (PEI, M_w = 70 000), polystyrenesulfonate (PSS, M_w = 70 000), poly(diallyldimethylammonium chloride) solution (PDADMAC), di(ethylene glycol) methyl ether methacrylate (MEO_2MA, M_n = 188), and oligo(ethylene glycol) methyl ether methacrylate (OEGMA, M_n = 475), were purchased from Aldrich and used without further purification. The macroinitiator MA01 was synthesized as described in a previous publication.[36] Prior to use, all the surfaces were cleaned by immersion in a solution of potassium permanganate in 100 mL of concentrated sulfuric acid for at least 1 h. ***Caution!*** *Sulfuric acid and permanganate solutions are dangerous and should be used with extreme care. Never store these solutions in closed containers.* The chemical structures of all the polymers used in this study are reported in Scheme S1 of the Supporting Information.

Purification of Decane. Decane was purchased from Aldrich and used after proper purification as described in ref 50. Briefly, 300 mL of decane were placed in a 500 mL separatory funnel with 30 mL of concentrated sulfuric acid, then the solution was vigorously shaken, and decane was decanted. The separation procedure was repeated three times; the solution was washed with Milli-Q water, then shaken twice with 30 mL of 2% NaOH solution, and washed again with Milli-Q water. After decane collection, the solution was dried over anhydrous Na_2SO_4 for 6 h. The solution was then transferred to a round-bottomed flask and distilled (under reflux) at 178 °C to remove residual water. ***Caution!*** *Handle hot glassware carefully.* Distilled decane was finally dried over activated Al_2O_3 in an Erlenmeyer flask for several hours. The aluminum oxide was then removed by filtration. The last step was repeated until the interfacial tension was close to the nominal decane/water interfacial tension ($\gamma \approx 52$ mN/m at room temperature).[51]

Fabrication of P(MEO_2MA-co-OEGMA) Coated Substrates. The thermoresponsive brushes P(MEO_2MA_x-*co*-$OEGMA_y$) were grown on layer-by-layer (LbL) structures according to the method described by Wischerhoff et al.[52] Briefly, multilayer structures were assembled on glass slides consisting of an alternating polyelectrolyte multilayer system with a nonlinear growth regime, a single macroinitiator layer, and the polymer brush grafted on the macroinitiator layer via surface-initiated atom transfer radical polymerization (SI-ATRP). The layer sequence was PEI/PSS/$(PDADMAC/PSS)_4$/PDADMAC/MA01/P(MEO_2MA_x-*co*-$OEGMA_y$). The polymers forming the multilayer structure were deposited from acidic solutions (pH = 1) containing 1.0 mg/mL of polymer and 0.5 M NaCl. The final multilayers were dried with a blower at 50 °C and then handled at ambient conditions. When not in use the samples were stored in a closed environment with desiccant at constant relative humidity of 40%.

A schematic of the brush architecture is reported in Scheme 1. The molar ratio of MEO_2MA to OEGMA was varied from (x/y) = 92:8 to 100:0 (mol/mol), and the time for SI-ATRP was 60 min. Layer thickness was measured by ellipsometry (described in detail in Wischerhoff et al.[52]); the thickness of PEI/PSS/$(PDADMAC/PSS)_4$/PDADMAC was δ = 62 ± 2 nm, the macroinitiator MA01 was δ = 12.5 ± 1 nm thick, and the grafted polymer brushes had thickness in the range of 50 < δ, nm < 60. Copolymer surface coverage has been estimated by ellipsometry, $\Gamma_{brush} \approx 53$ mg m^{-2} ($\Gamma_{brush} \approx 4.0 \times 10^{-7}$ mol m^{-2}).[53] The grafted brushes exhibited tunable LCST both in water and in PBS. PNIPAM thermoresponsive substrates were used as purchased from Thermo Scientific: Nunc 6-well multidishes with UpCell Surface.

2.2. Methods. *Water in Decane Contact Angle Experiments.* The wetting behavior of the thermoresponsive brushes was investigated by measuring the water in decane contact angle θ with a profile analysis tensiometer (PAT1, Sinterface, Germany) as a function of temperature in a sessile drop configuration. The temperatures were in the range of 20 < T, °C < 45, and they were controlled with a Haake thermostat with sensitivity to 0.1 °C.

Contact angle values were determined from the shape of the axisymmetric menisci using the axisymmetric drop shape analysis (ADSA) technique. Assuming that the experimental drop is Laplacian and axisymmetric, ADSA finds the theoretical profile that best matches the drop profile extracted from the image of a real drop, from which the surface tension, contact angle, drop volume, and surface area can be computed. The strategy employed is to fit the shape of an experimental drop to a theoretical drop profile according to the Laplace equation of capillarity, using the interfacial tension as an adjustable parameter. The best fit identifies the correct interfacial tension from which the contact angle can be determined by a numerical integration of the Laplace equation. Details of the methodology and experimental setup can be found in the works of Neumann et al.[54−56]

The experimental setup is reported in Scheme 1. The samples were placed on top of Teflon bars immersed in a quartz cuvette filled with purified decane. Typically, a water droplet (V = 20 μL) was formed at the tip of a needle and brought into contact with the surface. The needle was retracted from the droplet, and static contact angle was measured. For each temperature, contact angles were taken versus time until stability was reached (not more than 0.2° variation in 10 min). Contact angle equilibrium typically took from 1 to 3 h depending on the prior temperature jump. The equilibrium contact angle was taken as the average of the last 20 values obtained in the stable region. The relative precision and repeatability of the measurements in a given set of measurements is on the order of 0.3°. The reported values are the average ± standard error of at least three different replicates.

Ellipsometry. Layer thicknesses were determined on dry samples by null ellipsometry on a Multiscope (Optrel GbR, Kleinmachnow, Germany) with an angle of incidence of 70°. Film thicknesses were calculated, using a four-layer model (software Elli version 5.2, Optrel GbR) with the following parameters: layer one, air (n = 1.0000, k = 0); layer two, organic layer (n = 1.5000, k = 0); layer three, SiO_2 (d = 1.0 nm, n = 1.4580, k = 0); and layer four, silicon (n = 3.8858, k = −0.0200). On each sample, the measurements were performed on three randomly chosen spots; the reported thickness values represent averages derived from these measurements.

Atomic Force Microscopy. AFM experiments were carried out using a Park System XE-100 microscope (PSIA inc., Korea) controlled by the software XEP version 1.7. Typical contact mode AFM images were acquired at room temperature in air employing a silicon NSC36C tip (curvature radius less than 10 nm) with a force constant f = 0.6 N/m and frequency of 75 kHz. Both topography and lateral force channels were acquired. The scan rate was set to 0.8 Hz, and the Servo Gain was set to 1.2. All AFM pictures shown are height images unless

DOI: 10.1021/am507418m
ACS Appl. Mater. Interfaces 2015, 7, 2518−2528

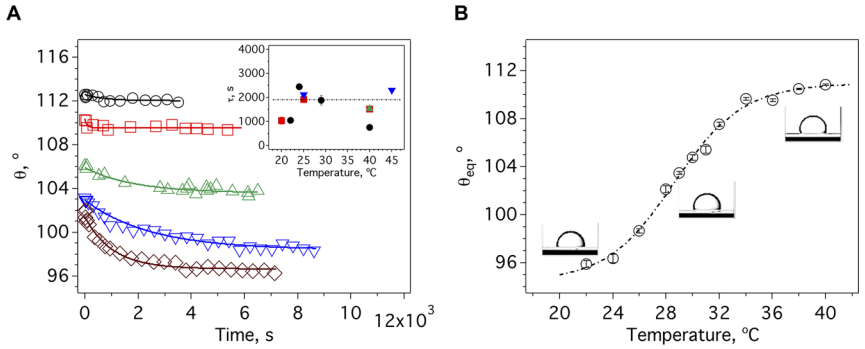

Figure 1. Temperature tunable wettability of P(MEO_2MA) brushes. (A) Water in decane contact angle θ against time: T = 22 (◇), 24 (▽), 29 (△), 34 (□), and 40 (○) °C. The solid lines are fitted to a single exponential function (eq 3). (inset) Characteristic relaxation time τ as a function of temperature and composition: P(MEO_2MA) (●), P(MEO_2MA_{97}-*co*-$OEGMA_3$) (■), P(MEO_2MA_{94}-*co*-$OEGMA_6$) (▲), P(MEO_2MA_{92}-*co*-$OEGMA_8$) (▼). (B) Contact angle values at equilibrium θ_{eq} as a function of temperature (○). The dashed line is a guide for the eyes.

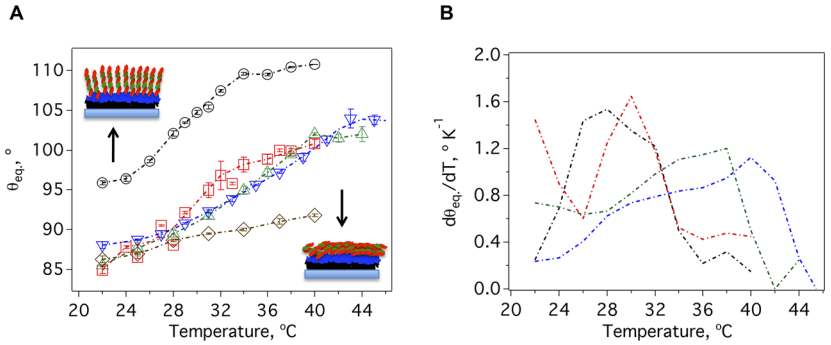

Figure 2. (A) Equilibrium contact angle values for the thermoresponsive brushes as a function of temperature: P(MEO_2MA) (○), P(MEO_2MA_{97}-*co*-$OEGMA_3$) (□), P(MEO_2MA_{94}-*co*-$OEGMA_6$) (△), P(MEO_2MA_{92}-*co*-$OEGMA_8$) (▽), and PNIPAM (◇). The dashed lines represent the linear interpolation to the data. (B) First derivative of the equilibrium contact angle with T for the P(MEO_2MA_x-*co*-$OEGMA_y$) brushes.

noted otherwise. All of the images shown are raw data processed only by flattening. Surface roughness (R_a), roughness factor (r_s), and height profiles of the samples were measured using WSxM software version 5.0 Develop 4.[57]

The average roughness was calculated as the arithmetic average of the height profiles, h_i.

$$R_a = \frac{1}{n}\sum_{i=1}^{n}|h_i| \quad \text{(eq 1)}$$

The roughness factor is defined as the ratio between the area of the actual surface (measured area) to that of a smooth surface having the same geometric shape and dimensions (geometric area).[58]

$$r_s = \frac{\text{actual surface}}{\text{geometric surface}} \quad \text{(eq 2)}$$

All the values here reported are the average of at least three different regions with comparable scan size and resolution.

Cell Culture and Imaging. Mouse fibroblast cells (L-929; ATCC CCL-1) were subcultured in Dulbecco's Modified Eagle's medium (Lonza) containing 10% fetal bovine serum (Hyclone, Thermo Scientific), 1% L-glutamine (Lonza), and 1% penicillin/streptomycin (Lonza) at 37 °C and 5% CO_2. Media was exchanged at 48 h intervals. To seed cells onto P(MEO_2MA-*co*-OEGMA) substrates, all samples were incubated in culture medium for 2 h, and cells were plated at a density of 25 000 cells/cm^2. All samples were imaged after 1 and 6 h of culture using a Nikon TS100 inverted microscope with 20× magnification.

Quantitative Cell Analysis. Phase contrast images (n = 6) were analyzed using NIS Elements Software (Nikon; Basic Research, Version 3.10). All cells with observable protrusions off of the cell body ("attached" cells) and those cells without protrusions ("not attached") were counted manually. Percent cell attachment was calculated as the ratio of attached cells over total cells. The area and perimeter of each cell was also obtained using NIS Elements, and the circularity of individual cells was calculated using $c = 4\pi\cdot\text{area/perimeter}^2$. Results are presented as averages ± standard deviation. Statistical analysis was performed in MINITAB 16 using one-way ANOVA with a posthoc Tukey's Test and 95% confidence interval.

3. RESULTS

3.1. Water−Decane−Solid Contact Angle for P(MEO_2MA_x-*co*-$OEGMA_y$) Brushes. The wettability of P(MEO_2MA_x-*co*-$OEGMA_y$) brushes with 100:0 < (x/y) < 92:8 for 20 < T, °C < 45 was studied by measuring water−decane−solid contact angle θ using profile analysis tensiometry, as described in the Methods Section. Figure 1A shows the variation of contact angle as a function of time for P(MEO_2MA) (x/y = 100:0) brushes at selected temperatures.

The contact angle shows a decrease as a function of time. For y = 0, that is, P(MEO_2MA), the time to reach a stable contact angle value θ_{eq} increases with cooling: from 30 min for T = 40 °C to more than 2 h for T = 22 °C, suggesting temperature-dependent kinetics for the observed process. Although at high temperatures the decrease of contact angle is negligible and the kinetics are relatively fast, at T = 22 °C we observe as much as 5% decrease in contact angle. Representative data for other copolymer (x/y) compositions are reported in Figure S1 of the Supporting Information. To describe the evolution of the water contact angle, the measured $\theta(t)$ was compared to the simplest realistic macromolecular relaxation model. The Kelvin−Voigt model for viscoelastic materials, that is, a spring and damper in

DOI: 10.1021/am507418m
ACS Appl. Mater. Interfaces 2015, 7, 2518−2528

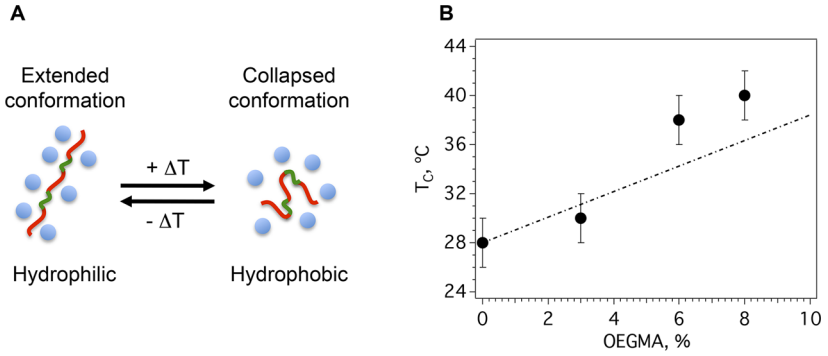

Figure 3. (A) Schematic of the hydrophilic to hydrophobic transition. (B) Critical temperature T_C as a function of the OEGMA/MEO_2MA molar ratio (●). Data are obtained from the maxima of $d\theta_{eq}/dT$ vs T profiles shown in Figure 2B. The dashed line is the linear relationship between LCST and OEGMA units in solution according to Lutz et al.:[60] LCST = 28° + 1.04·OEGMA(%).

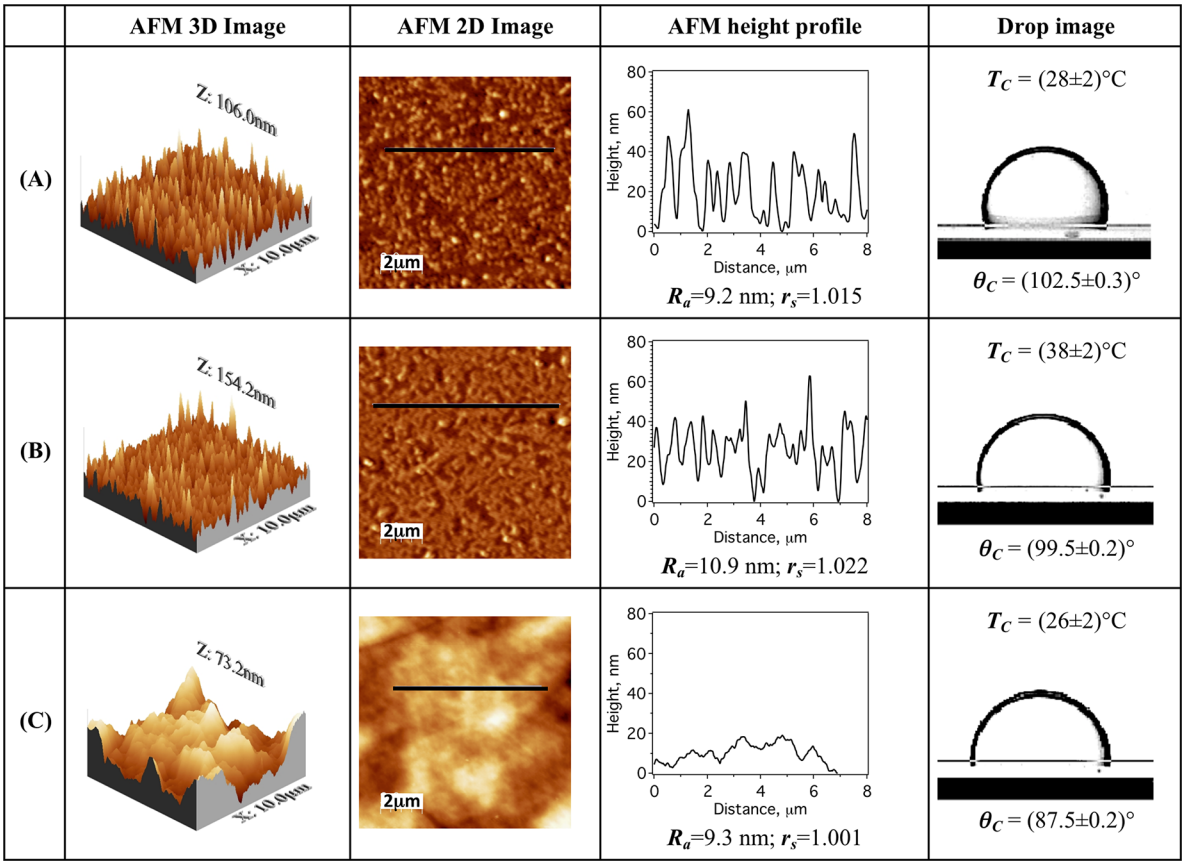

Figure 4. Atomic force microscopy and water-in-decane contact angle at T_C, θ_C for (a) P(MEO_2MA), (b) P(MEO_2MA_{94}-*co*-$OEGMA_6$), and (c) UpCell PNIPAM brushes. AFM scan size: 10 μm × 10 μm. Below the AFM profile, both the average surface roughness R_a and the roughness ratio r_s are indicated. Volume of the water drop V = 20 μL.

series,[59] describes the surface relaxation dynamics by a single exponential function.

$$\frac{\theta(t) - \theta_0}{\theta_{eq} - \theta_0} = (1 - \exp(-t/\tau)) \quad \text{(eq 3)}$$

where θ_0 is the contact angle value at time $t \approx 0$ s, and τ is the material-dependent time constant. As shown in Figure 1A, the experimental data satisfactorily fit the selected function. Interestingly, the relaxation time constant is nearly independent of both temperature and composition, $\tau \approx 1900$ s, see the inset of Figure 1A, which is expected for ideal macromolecules of the same molecular weight. This time constant is quantitatively similar to the observation of Kessel et al. (2010), t = 20 min, for the time-dependent adhesion study on P(MEO_2MA_{90}-*co*-$OEGMA_{10}$)-coated surfaces.[32]

The behavior of the equilibrium contact angle θ_{eq} for (x/y) = 100:0 is reported in Figure 1B for each temperature examined. A decrease of contact angle is observed upon cooling; that is, hydrophilicity increases while decreasing temperature. Because the contact angles for the polyelectrolyte prelayer interface (PEI/PSS/$(PDADMAC/PSS)_4$/PDADMAC) and for the bare supports do not change for these temperatures within experimental error (data not shown), it is evident that these variations result from the change in the interfacial properties of the P(MEO_2MA) layer.

DOI: 10.1021/am507418m
ACS Appl. Mater. Interfaces 2015, 7, 2518−2528

Similar considerations may be drawn for the other three systems; the wetting behavior of P(MEO_2MA_x-*co*-$OEGMA_y$) brushes with different (x/y) copolymer ratios are shown in Figure 2A against temperature. The thermoresponsive wetting behavior of UpCell substrates was also measured and shown for reference.

We always observed an increase in contact angle with temperature increase; that is, hydrophobicity increases upon heating. Ethylene oxide (EO) methacrylate-based polymers show a higher response to temperature with respect to the UpCell surface; for P(MEO_2MA_x-*co*-$OEGMA_y$)-coated substrates the maximum change of contact angle is $\Delta\theta_{eq} \approx 15°$, while in the case of UpCell brushes $\Delta\theta_{eq} \approx 6°$. We also found the P($MEO_2MA$) brush is the most hydrophobic polymer: for almost all the temperatures examined, θ_{eq} is ~10° higher than the other samples. Interestingly, except for 100% MEO_2MA, decreasing the MEO_2MA/OEGMA ratio results in only a slight variation in contact angle, suggesting that the ethylene glycol (hydrophilic) units are much more exposed to the solid/water interface with respect to the methacrylate (hydrophobic) backbone.

Further details on the switchable wettability of P(MEO_2MA_x-*co*-$OEGMA_y$) brushes are shown in Figure 2B where the first derivative of the equilibrium contact angle $d\theta_{eq}/dT$ against temperature is reported for different copolymer ratios. The maxima in the $d\theta_{eq}/dT$ versus T profiles shift to higher temperatures with increasing OEGMA content, indicating a composition-dependent switching behavior.

The contact angle data for the P(MEO_2MA_x-*co*-$OEGMA_y$) brushes show no sharp change at any point. We therefore hypothesize that with increasing temperature, the polymer undergoes a cooperative conformational transition between a hydrophilic (swollen brush) to a hydrophobic (collapsed coil) state (see Figure 3A), as suggested also by Zhulina et al.[61] and observed by other authors.[62]

The phase transition temperature of the brushes T_C was detected from the maxima in the $d\theta_{eq}/dT$ versus T profiles shown in Figure 2B. We found T_C increases almost linearly with the OEGMA/MEO_2MA ratio, in accordance with the LCST measured by Lutz et al. for P(MEO_2MA_x-*co*-$OEGMA_y$) in aqueous suspensions[60]—see Figure 3B.

3.2. Atomic Force Microscopy Study for P(MEO_2MA_x-*co*-$OEGMA_y$) Brushes. Surface roughness and morphology for P(MEO_2MA_x-*co*-$OEGMA_y$) brushes were analyzed by AFM experiments. Height images of P(MEO_2MA), P(MEO_2MA_{94}-*co*-$OEGMA_6$), and UpCell PNIPAM substrates are compared in Figure 4.

The P(MEO_2MA_x-*co*-$OEGMA_y$)@SiO_2 substrates show densely packed surfaces with similar roughness ($R_a \approx$ 10nm) and thickness ($\delta \approx$ 30−50nm); PNIPAM surface (UpCell) appears less structured with an average thickness, $\delta \approx$ 15nm. For nonideal surfaces, such as polymer-coated substrates, the morphology affects the wettability of a surface. In this case, the apparent contact angle θ^* can be described by the Wenzel equation[63]

$$\cos\theta^* = r_s \cos\theta_i \qquad \text{(eq 4)}$$

where r_s is the roughness factor defined by equation (eq 2) and θ_i is the true contact angle of the polymer brush. From the AFM analysis we obtain an average roughness factor r_s = 1.02; hence, the measured contact angles for the P(MEO_2MA_x-*co*-$OEGMA_y$) brushes can be considered ideal under the experimental error. In this latter case, despite similarities in the morphology of the substrates, we show measurable differences in their hydrophilic-to-lipophilic balance (HBL). At the critical temperature T_C of the polymer brushes we observe a variation of 3° in contact angle, corresponding to a surface energy variation, $\Delta G/A \approx 0.5$ mJ/m^2 × OEGMA (%).

3.3. Cell Spreading on P(MEO_2MA_x-*co*-$OEGMA_y$) Brushes. Because of the observed differences in the HBL for the P(MEO_2MA_x-*co*-$OEGMA_y$) brushes, attachment of fibroblast cells was utilized as a tool to demonstrate the effect of contact angle variation on substrates with different surface composition on cell adhesion. Scheme 2 shows the methodology of cell attachment and detachment as a function of temperature on the thermoresponsive brushes.

Scheme 2. Cell Attachment (top) and Thermorelease (bottom) on P(MEO_2MA_x-*co*-$OEGMA_y$) Brushes Grafted on LbL Structure[a]

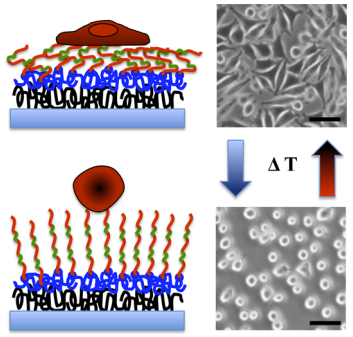

[a]Cells adhere to thermobrushes at 37°C above the LCST and detach after 20 min at 23°C below the LCST. Scale bar is 50 μm.

Initial cell attachment and cell morphology was assessed after 1 h using phase contrast microscopy for cells cultured on P(MEO_2MA_x-*co*-$OEGMA_y$) brushes at 37 °C. Figure 5 shows that initial cell attachment on P(MEO_2MA-*co*-OEGMA) brushes decreases with increasing OEGMA content (Figure 5A−D). Observed cell attachment was robust on UpCell substrates, which are used as the thermoresponsive "gold standard" in current cell culture applications (Figure 5E).

The progression of cell spreading on the various substrates is compared after 6 h in Figure 6. Cell attachment was quantified manually using observable cell protrusions (Figure 6A). Cell attachment was significantly greater on UpCell PNIPAM substrates than on P(MEO_2MA-*co*-OEGMA) brushes. Surfaces with greater amounts of OEGMA (6 and 8%) supported the lowest degree of cell attachment. Importantly, although there is a lag in initial cell attachment rates across substrates, all surfaces supported cell proliferation, as there was no statistical difference in cell number after 48 h of culture (data not shown). Figure 6B quantifies cell circularity, which is indicative of cell spreading: the lower the circularity metric, the more spread (less circular) are the cells. There is no difference in the cell spreading, or morphology, between PNIPAM and P(MEO_2MA). There is an observed increase in circularity as OEGMA% increases.

4. DISCUSSION

The overall analysis of the data shows the polymer surface chemistry plays a dominant role in the wetting behavior of thermoresponsive substrates and systematically influences cell adhesion under physiological conditions. In particular, compar-

DOI: 10.1021/am507418m
ACS Appl. Mater. Interfaces 2015, 7, 2518−2528

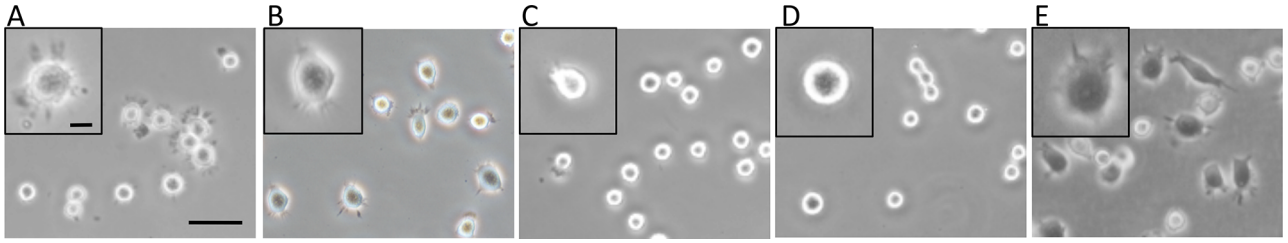

Figure 5. Initial L929 fibroblast attachment on thermoresponsive brushes after 1 h. (A) P(MEO_2MA), (B) P(MEO_2MA_{97}-*co*-$OEGMA_3$), (C) P(MEO_2MA_{94}-*co*-$OEGMA_6$), (D) P(MEO_2MA_{92}-*co*-$OEGMA_8$), and (E) UpCell PNIPAM substrates. Inset scale bar is 10 μm. Scale bar is 50 μm.

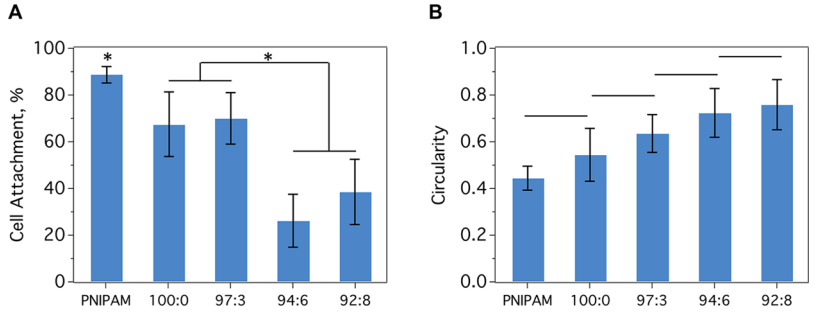

Figure 6. Average fibroblast attachment (A) and circularity (B) on P(MEO_2MA_x-*co*-$OEGMA_y$) and UpCell PNIPAM substrates after 6 h. * indicates $P < 0.05$; experimental data bars that share significance are grouped together; otherwise, data are significant at $P < 0.05$.

Table 1. OEGMA Areal Fraction f_y and Solid−Decane Interfacial Energy γ_{br}^{D} for P(MEO_2MA_x-*co*-$OEGMA_y$)-Coated Substrates at T = 22 °C, T = LCST, and T = 37 °C

	f_y			γ_{br}^{D}, mJ/m^2		
composition (x/y)	T = 22 °C	T = LCST	T = 37 °C	T = 22 °C	T = LCST	T = 37 °C
100:0				17.5	14.0	10.4
97:3	0.72 ± 0.24	0.56 ± 0.06	0.35 ± 0.11	19.7	15.4	13.0
94:6	0.68 ± 0.19	0.47 ± 0.02	0.38 ± 0.09	19.9	14.6	13.2
92:8	0.52 ± 0.12	0.41 ± 0.07	0.41 ± 0.07	18.7	13.7	13.7

ison of contact angle data and AFM measurements suggests cellular adhesion and/or uptake depends on the specific HBL balance of the polymer brush rather than the nature of the support or the surface morphology.

The wetting kinetics is only marginally affected by the copolymer composition or temperature. In all cases we observed an exponential decrease of contact angle with time increase. The amount of this decrease may depend on several factors such as macromolecular conformational changes, water adsorption to, spreading on, or diffusion through the polymer chains. Our experimental data and observations do not exclude any of these phenomena, so it is difficult to draw thoughtful conclusions on the wetting kinetics; this is beyond the scope of our intentions in the manuscript.

Despite uncertainties in the nature of the overall wetting kinetics, we found the relaxation time to be nearly independent of both temperature and composition, with $\tau \approx 30$ min. This value is in good agreement with the hydrophobic-to-hydrophilic adhesion switching time observed by Kessel et al. (2010) for P(MEO_2MA_x-*co*-$OEGMA_y$)-coated on gold surfaces by using colloidal probe AFM ($t \approx 20$ min).[32] Thus we hypothesize time-dependent conformational changes are present at the macromolecular surface.

We show the hydrophilic-to-hydrophobic transition can be controlled by varying both the temperature of the fluid phase and the copolymer (x/y) ratio. Independent of the composition, we observe an average decrease in contact angle $\Delta\theta \approx 13°$ upon cooling from T = 37 °C to room temperature T = 22 °C. However, the inflection point in the θ_{eq} versus T profiles shifts to higher temperatures as the ethyleneglycol fraction (y = OEGMA) in the copolymer chains increases. A compositional variation of air−water contact angle for P(MEO_2MA_x-*co*-$OEGMA_y$) brushes was previously observed by Jonas et al. (2007) using a captive bubble configuration.[35] In this case, the LCST was determined from the fitting of the $\theta(T)$ data using an empirical second-order polynomial equation. However, more recent studies on the surface wettability of P(MEO_2MA_x-*co*-$OEGMA_y$)-coated substrates showed controversial results. For example, Dey et al. (2011) noticed a thermoresponsive behavior for the air−water contact angle of P(MEO_2MA_{90}-*co*-$OEGMA_{10}$) coated on glass substrates (from $\theta = 50°$ at T = 20 °C to $\theta = 64°$ at T = 37 °C),[64] while Uhlig et al. (2012) did not observe such changes using the same copolymer system, $\theta \approx 55°$.[53] We ascribe the disagreement to the measurement configuration used (water contact angle in air) and/or difference in the preparation protocol.

To quantify the effect of composition on the wetting behavior of the thermoresponsive brushes we applied the Cassie−Baxter equation to the experimentally measured contact angle values. Cassie's law describes the effective contact angle θ_c for a liquid on a composite surface.[65] Assuming the P(MEO_2MA_x-*co*-$OEGMA_y$)-coated surface as a two-component system, the effective contact angle can be described as

DOI: 10.1021/am507418m
ACS Appl. Mater. Interfaces 2015, 7, 2518−2528

$$\cos(\theta_c) = f_x \cos(\theta_x) + f_y \cos(\theta_y) \quad \text{(eq 5)}$$

where θ_x is the contact angle for MEO_2MA with areal fraction f_x, and θ_y is the contact angle for OEGMA with areal fraction $f_y = (1 - f_x)$ present at the solid/water interface. This assumption is based on previous findings where it was demonstrated that although P(MEO_2MA-*co*-OEGMA) and other oligoethylene-glycol-based copolymers are random, side OEG units are flexible enough to undergo phase separation.[33,66] Here, the OEGMA areal fraction, f_y, was calculated by solving eq 5 for all (x/y) copolymer ratios and 22 <T, °C < 40, keeping constant the OEGMA contact angle value, θ_y, and using the experimental contact angle values for both composites and the P-(MEO_2MA)-coated substrate. The contact angle of P-(OEGMA) (x/y = 0:100) can be considered constant since the investigated temperatures are much below the LCST of the polymer, $T \ll$ LCST = 90 °C.[60] From the fitting of the data we found a value of θ_y = 80.6° as the confined OEGMA contact angle; the calculated OEGMA areal fractions are shown in Table 1 for different temperatures and copolymer compositions. Our analysis evidence that f_y is only slightly affected, that is, less than the experimental error, by the nominal (x/y) molar ratio, signifying that in a narrow range of copolymer compositions (3 <y, % < 8) the P(MEO_2MA_x-*co*-$OEGMA_y$)-coated substrates exhibits similar hydrophilicity.

Independent of the composition, the areal fraction of OEGMA, and hence the hydrophilicity, increases from f_y = 0.4 to f_y = 0.7 upon cooling. Because the (x/y) molar ratio does not change with a temperature variation, this finding suggests that the cooling process leads to a macromolecular conformational change, which increases the number of ethylene glycol (hydrophilic) units exposed to the solid/water interface. More information is reported in Figure S2 of the Supporting Information, where the plot of f_y versus T is shown for all the compositions.

Further details on the temperature-dependent wettability of P(MEO_2MA_x-*co*-$OEGMA_y$) brushes can be obtained from the analysis of their surface energy with respect to decane. The brush/decane interfacial energy γ_{SD} is defined by Young's equation[67] as

$$\gamma_{br}^{D} = \gamma_{br}^{W} + \gamma_{WD} \cos\theta_{eq} \quad \text{(eq 6)}$$

where γ_{br}^{W} and γ_{WD} refer to the brush/water and water/decane interfacial tension, respectively. If $\gamma_{br}^{D} < \gamma_{br}^{W} + \gamma_{WD}$ a droplet of finite size contact angle minimizes the free energy of the system, and the water will spread over the substrate. On the other hand, if $\gamma_{br}^{D} = \gamma_{br}^{W} + \gamma_{WD}$ the contact angle is zero; the system will be in equilibrium when water completely wets the interface.

Here, the brush/decane interfacial energy γ_{br}^{D} was calculated according to the method proposed by Li and Neumann:[68]

$$\cos\theta_{eq} = -1 + 2\sqrt{\frac{\gamma_{br}^{D}}{\gamma_{WD}}}\, e^{-\beta(\gamma_{WD}-\gamma_{br}^{D})^2} \quad \text{(eq 7)}$$

where β = 0.000 1247 $(m/mN)^2$ was determined from an averaging process on different surfaces.[69] For measured values of θ_{eq} and γ_{WD} the value of γ_{br}^{D} can be calculated by an iterative method from eq 7. Results from the iteration process are reported in Table 1 for all the examined (x/y) molar ratios and different temperatures. Independent of the composition the surface energy increases more than 30% upon cooling from T = 37 to 22 °C, reflecting the same trend with temperature as the OEGMA areal fraction. Below and above the critical temperature of the copolymer, the surface energy for P(MEO_2MA)-coated substrates is ~3 mJ/m^2 lower than the other compositions, while at T = LCST the brush/decane surface energy is nearly unaffected by the composition, γ_{br}^{D} = 14.4 ± 0.4 mJ/m^2.

Although several studies have reported on the effects of hydrophobicity or wettability on cell attachment,[53,64,70] direct comparisons are difficult to make due to differences in the thermoresponsive surface preparation (variable grafting density, morphology, etc.) and the surface characterization techniques (method of contact angle and AFM measurements). Here, we compare side by side the effects of (x/y) ratio on the surface energy of P(MEO_2MA_x-*co*-$OEGMA_y$) brushes. The results demonstrate that surface energy can be incrementally modified by increasing the percentage of OEGMA monomers in the thermoresponsive copolymer, which has a direct effect on the biological process of cell attachment or, more generally, biological adhesion. Under culture conditions at 37 °C, the brush/decane interfacial energy γ_{SD} is much lower for (x/y) = 100:0 (10.4 mJ/m^2) than the copolymers containing 3−8% OEGMA (γ_{br}^{D} = 13.0−13.7 mJ/m^2), and the copolymers show an incremental increase in interfacial energy as OEGMA content increases. Initial cell attachment is greatest on the P(MEO_2MA) surface with the lowest interfacial energy (i.e., γ_{br}^{D}). As this energy increases, initial cell attachment decreases (Figure 5). This result is independent of surface morphology of the brush surface, as there was no observed difference in morphology or brush height as a function of (x/y) on P(MEO_2MA_x-*co*-$OEGMA_y$) brushes as observed by ellipsometry and AFM (Figure 4). Joy et al. (2010) reported similar results in a study that used a library of methacrylate terpolymers to explore the effects of varying surface chemistry on cell attachment. The work demonstrated that the composition of the polymers influences cell behavior (attachment and proliferation), with the strongest correlation being between contact angle and the cell response.[70]

UpCell was included in the study only as a reference due to its use as the current gold standard of thermoresponsive cell culture substrates. UpCell (PNIPAM), however, is different both morphologically and chemically, so it is inappropriate to compare UpCell surfaces directly to the tunable P(MEO_2MA_x-*co*-$OEGMA_y$) brushes characterized in this study.

5. CONCLUSIONS

Controlling the adhesive properties of stimulus-responsive surfaces is critical to the success of these surfaces as substrates capable of reversible adhesion; in this particular example, mammalian cell attachment and detachment. We prepared a homologous series of thermoresponsive substrates based on random copolymers of 2-(2-methoxyethoxy)ethyl methacrylate (x = MEO_2MA) and oligo(ethylene glycol) methacrylate (y = OEGMA), namely, P(MEO_2MA_x-*co*-$OEGMA_y$), grown on planar LbL architectures to investigate the role of morphology and surface chemistry on wetting and adhesion phenomena at solid/fluid interfaces. We demonstrate the ability to incrementally modify the surface energetics of P(MEO_2MA_x-*co*-$OEGMA_y$) brushes by varying the percentage of OEGMA monomers in the polymer chains. Switchable wettability and adhesion have been achieved by means of water−decane contact angle measurements and modulated by varying the copolymer 92:8 < x/y < 100:0 ratio and the external temperature 20 < T, °C < 45.

DOI: 10.1021/am507418m
ACS Appl. Mater. Interfaces 2015, 7, 2518−2528

While the morphology of the substrates seems to be unaffected by the x/y ratio, the polymer composition plays a key role in surface wettability. Independent of the composition the equilibrium contact angle θ_{eq} decreases (hydrophilicity increases), while cooling below the LCST of the copolymer brushes indicates a temperature-dependent conformational change of the polymer/water interfacial layer. Increasing the OEGMA content on the copolymer brush, the contact angle versus T profiles shift to higher temperatures with P-(MEO_2MA) being the most hydrophobic system. Similarly, the surface energy of the substrates (γ_{br}^{D}) significantly increases with cooling and with increasing the percentage of OEGMA in the copolymer brush. We ascribe these phenomena to the phase transition between the hydrophobic and the hydrophilic states of P(MEO_2MA_x-*co*-$OEGMA_y$) copolymers.

Using our experimental findings we extracted the underlying energetics associated with liquid-liquid-solid adhesion as a function of the copolymer ratio. In accordance with previous works in solution we found a linear relationship between the x/y ratio and the LCST. The alteration of contact angle and thus the energy of the surfaces resulted in differential cell attachment as a function of surface hydrophobicity.

These results enhance our understanding of the physical principles that rule wetting phenomena and will allow for the improved design of engineered dynamic surfaces capable of reversible adhesion properties in real-time in response to external stimuli.

■ ASSOCIATED CONTENT

Ⓢ Supporting Information

Illustrated chemical structures of polyions used in the present work; wetting kinetics and OEGMA areal fraction against temperature for P(MEO_2MA_x-*co*-$OEGMA_y$)-coated substrates. This material is available free of charge via the Internet at http://pubs.acs.org.

■ AUTHOR INFORMATION

Corresponding Author

*Phone: +1(610) 330-5820. Fax +1(610) 330-5059. E-mail: ferrij@lafayette.edu.

Notes

The authors declare no competing financial interest.

■ ACKNOWLEDGMENTS

Financial support from National Aeronautics and Space Administration (NASA)/Glenn Research Center (Particle Stabilized Emulsions and Foams, Award No. NNX10AV26G) in cooperation with the European Space Administration (ESA) through Opportunity No. AO-2009-0813 and the Camille and Henry Dreyfus Foundation is acknowledged. The authors thank K. Ling for contributing to contact angle measurements, T. Fruneaux for assistance with quantitative cell analysis, and the Center for Colloid and Surface Science (Florence, Italy) for the utilization of AFM facilities.

■ REFERENCES

(1) Yao, X.; Song, Y.; Jiang, L. Applications of Bio-Inspired Special Wettable Surfaces. *Adv. Mater.* **2011**, *23*, 719−734.

(2) Feng, L.; Zhang, Z.; Mai, Z.; Ma, Y.; Liu, B.; Jiang, L.; Zhu, D. A Super-Hydrophobic and Super-Oleophilic Coating Mesh Film for the Separation of Oil and Water. *Angew. Chem., Int. Ed.* **2004**, *43*, 2012−2014.

(3) Garrod, R. P.; Harris, L. G.; Schofield, W. C. E.; McGettrick, J.; Ward, L. J.; Teare, D. O. H.; Badyal, J. P. S. Mimicking a Stenocara Beetle's Back for Microcondensation Using Plasmachemical Patterned Superhydrophobic−Superhydrophilic Surfaces. *Langmuir* **2006**, *23*, 689−693.

(4) Daniel, S.; Chaudhury, M. K.; Chen, J. C. Fast Drop Movements Resulting from the Phase Change on a Gradient Surface. *Science* **2001**, *291*, 633−636.

(5) Caminati, G. Cultural Heritage Artefacts and Conservation: Surfaces and Interfaces. In *Nanoscience for the Conservation of Works of Art;* The Royal Society of Chemistry: Cambridge, U.K., 2013; Vol. *1*, pp 1-48.

(6) Liu, M.; Zheng, Y.; Zhai, J.; Jiang, L. Bioinspired Super-antiwetting Interfaces with Special Liquid−Solid Adhesion. *Acc. Chem. Res.* **2009**, *43*, 368−377.

(7) Chen, L.; Liu, M.; Bai, H.; Chen, P.; Xia, F.; Han, D.; Jiang, L. Antiplatelet and Thermally Responsive Poly(N-isopropylacrylamide) Surface with Nanoscale Topography. *J. Am. Chem. Soc.* **2009**, *131*, 10467−10472.

(8) Bhushan, B.; Jung, Y. C.; Koch, K. Self-Cleaning Efficiency of Artificial Superhydrophobic Surfaces. *Langmuir* **2009**, *25*, 3240−3248.

(9) Zhang, L.; Zhao, N.; Xu, J. Fabrication and Application of Superhydrophilic Surfaces: a Review. *J. Adhes. Sci. Technol.* **2012**, *28*, 769−790.

(10) Rauscher, M.; Dietrich, S. Wetting Phenomena in Nanofluidics. *Annu. Rev. Mater. Res.* **2008**, *38*, 143−172.

(11) Delamarche, E.; Juncker, D.; Schmid, H. Microfluidics for Processing Surfaces and Miniaturizing Biological Assays. *Adv. Mater.* **2005**, *17*, 2911−2933.

(12) Ionov, L.; Houbenov, N.; Sidorenko, A.; Stamm, M.; Minko, S. Smart Microfluidic Channels. *Adv. Funct. Mater.* **2006**, *16*, 1153−1160.

(13) Kubus, L.; Erdogan, H.; Piskin, E.; Demirel, G. Controlling Unidirectional Wetting via Surface Chemistry and Morphology. *Soft Matter* **2012**, *8*, 11704−11707.

(14) Minko, S.; Müller, M.; Motornov, M.; Nitschke, M.; Grundke, K.; Stamm, M. Two-Level Structured Self-Adaptive Surfaces with Reversibly Tunable Properties. *J. Am. Chem. Soc.* **2003**, *125*, 3896−3900.

(15) Xu, L.; Chen, W.; Mulchandani, A.; Yan, Y. Reversible Conversion of Conducting Polymer Films from Superhydrophobic to Superhydrophilic. *Angew. Chem., Int. Ed.* **2005**, *44*, 6009−6012.

(16) Mano, J. F. Stimuli-Responsive Polymeric Systems for Biomedical Applications. *Adv. Eng. Mater.* **2008**, *10*, 515−527.

(17) Ista, L. K.; Mendez†, S.; Lopez, G. P. Attachment and detachment of bacteria on surfaces with tunable and switchable wettability. *Biofouling* **2009**, *26* (1), 111−118.

(18) Falconnet, D.; Csucs, G.; Michelle Grandin, H.; Textor, M. Surface Engineering Approaches to Micropattern Surfaces for Cell-based Assays. *Biomaterials* **2006**, *27*, 3044−3063.

(19) Tirrell, M.; Kokkoli, E.; Biesalski, M. The Role of Surface Science in Bioengineered Materials. *Surf. Sci.* **2002**, *500*, 61−83.

(20) Okano, T.; Yamada, N.; Okuhara, M.; Sakai, H.; Sakurai, Y. Mechanism of Cell Detachment from Temperature-Modulated, Hydrophilic−Hydrophobic Polymer Surfaces. *Biomaterials* **1995**, *16*, 297−303.

(21) Canavan, H. E.; Cheng, X.; Graham, D. J.; Ratner, B. D.; Castner, D. G. Cell Sheet Detachment Affects the Extracellular Matrix: A Surface Science Study Comparing Thermal Liftoff, Enzymatic, and Mechanical Methods. *J. Biomed. Mater. Res., Part A* **2005**, *75A*, 1−13.

(22) Yamada, N.; Okano, T.; Sakai, H.; Karikusa, F.; Sawasaki, Y.; Sakurai, Y. Thermo-responsive Polymeric Surfaces; Control of Attachment and Detachment of Cultured Cells. *Makromol. Chem., Rapid. Commun.* **1990**, *11*, 571−576.

(23) Cooperstein, M. A.; Canavan, H. E. Assessment of Cytotoxicity of (*N*-Isopropyl acrylamide) and Poly(*N*-isopropyl acrylamide)-Coated Surfaces. *Biointerphases* **2013**, *8*, 19.

(24) Kano, M.; Kokufuta, E. On the Temperature-Responsive Polymers and Gels Based on N-Propylacrylamides and N-Propylmethacrylamides. *Langmuir* **2009**, *25*, 8649−8655.

DOI: 10.1021/am507418m
ACS Appl. Mater. Interfaces 2015, 7, 2518−2528

(25) Tsuda, Y.; Kikuchi, A.; Yamato, M.; Sakurai, Y.; Umezu, M.; Okano, T. Control of Cell Adhesion and Detachment Using Temperature and Thermoresponsive Copolymer Grafted Culture Surfaces. *J Biomed. Mater. Res., Part A* **2004**, *69A*, 70−78.
(26) Allen, L. T.; Fox, E. J. P.; Blute, I.; Kelly, Z. D.; Rochev, Y.; Keenan, A. K.; Dawson, K. A.; Gallagher, W. M. Interaction of Soft Condensed Materials with Living Cells: Phenotype/transcriptome Correlations for the Hydrophobic Effect. *Proc. Natl. Acad. Sci. U.S.A.* **2003**, *100*, 6331−6336.
(27) Lynch, I.; Blute, I. A.; Zhmud, B.; MacArtain, P.; Tosetto, M.; Allen, L. T.; Byrne, H. J.; Farrell, G. F.; Keenan, A. K.; Gallagher, W. M.; Dawson, K. A. Correlation of the Adhesive Properties of Cells to N-Isopropylacrylamide/*N*-*tert*-Butylacrylamide Copolymer Surfaces with Changes in Surface Structure Using Contact Angle Measurements, Molecular Simulations, and Raman Spectroscopy. *Chem. Mater.* **2005**, *17*, 3889−3898.
(28) Curtis, A. S. G.; Forrester, J. V.; Clark, P. Substrate Hydroxylation and Cell Adhesion. *J. Cell Sci.* **1986**, *86*, 9−24.
(29) Lindblad, M.; Lestelius, M.; Johansson, A.; Tengvall, P.; Thomsen, P. Cell and Soft Tissue Interactions with Methyl- and Hydroxyl-Terminated Alkane Thiols on Gold Surfaces. *Biomaterials* **1997**, *18*, 1059−1068.
(30) Lutz, J.-F.; Akdemir, Ö.; Hoth, A. Point by Point Comparison of Two Thermosensitive Polymers Exhibiting a Similar LCST: Is the Age of Poly(NIPAM) Over? *J. Am. Chem. Soc.* **2006**, *128*, 13046−13047.
(31) Zou, Y.; Rossi, N. A. A.; Kizhakkedathu, J. N.; Brooks, D. E. Barrier Capacity of Hydrophilic Polymer Brushes To Prevent Hydrophobic Interactions: Effect of Graft Density and Hydrophilicity. *Macromolecules* **2009**, *42*, 4817−4828.
(32) Kessel, S.; Schmidt, S.; Müller, R.; Wischerhoff, E.; Laschewsky, A.; Lutz, J.-F. o.; Uhlig, K.; Lankenau, A.; Duschl, C.; Fery, A. Thermoresponsive PEG-Based Polymer Layers: Surface Characterization with AFM Force Measurements. *Langmuir* **2009**, *26*, 3462−3467.
(33) Synytska, A.; Svetushkina, E.; Puretskiy, N.; Stoychev, G.; Berger, S.; Ionov, L.; Bellmann, C.; Eichhorn, K.-J.; Stamm, M. Biocompatible Polymeric Materials with Switchable Adhesion Properties. *Soft Matter* **2010**, *6*, 5907−5914.
(34) Lutz, J.-F. Thermo-Switchable Materials Prepared Using the OEGMA-Platform. *Adv. Mater.* **2011**, *23*, 2237−2243.
(35) Jonas, A. M.; Glinel, K.; Oren, R.; Nysten, B.; Huck, W. T. S. Thermo-Responsive Polymer Brushes with Tunable Collapse Temperatures in the Physiological Range. *Macromolecules* **2007**, *40*, 4403−4405.
(36) Wischerhoff, E.; Uhlig, K.; Lankenau, A.; Börner, H. G.; Laschewsky, A.; Duschl, C.; Lutz, J.-F. Controlled Cell Adhesion on PEG-Based Switchable Surfaces. *Angew. Chem., Int. Ed.* **2008**, *47*, 5666−5668.
(37) Ishida, N.; Kobayashi, M. Interaction Forces Measured between Poly(*N*-Isopropylacrylamide) Grafted Surface and Hydrophobic Particle. *J. Colloid Interface Sci.* **2006**, *297*, 513−519.
(38) Malham, I. B.; Bureau, L. Density Effects on Collapse, Compression, and Adhesion of Thermoresponsive Polymer Brushes. *Langmuir* **2009**, *26*, 4762−4768.
(39) Svetushkina, E.; Puretskiy, N.; Ionov, L.; Stamm, M.; Synytska, A. A Comparative Study on Switchable Adhesion between Thermoresponsive Polymer Brushes on Flat and Rough Surfaces. *Soft Matter* **2011**, *7*, 5691−5696.
(40) Ramiasa, M.; Ralston, J.; Fetzer, R.; Sedev, R. The Influence of Topography on Dynamic Wetting. *Adv. Colloid Interface Sci.* **2014**, *206*, 275−293.
(41) Genzer, J. Surface-Bound Gradients for Studies of Soft Materials Behavior. *Annu. Rev. Mater. Res.* **2012**, *42*, 435−468.
(42) Bonn, D.; Eggers, J.; Indekeu, J.; Meunier, J.; Rolley, E. Wetting and Spreading. *Rev. Mod. Phys.* **2009**, *81*, 739−805.
(43) Phillips, K. R.; Vogel, N.; Burgess, I. B.; Perry, C. C.; Aizenberg, J. Directional Wetting in Anisotropic Inverse Opals. *Langmuir* **2014**, *30*, 7615−7620.
(44) Lai, C. Q.; Thompson, C. V.; Choi, W. K. Uni-, Bi-, and Tri-Directional Wetting Caused by Nanostructures with Anisotropic Surface Energies. *Langmuir* **2012**, *28*, 11048−11055.
(45) Gambinossi, F.; Chanana, M.; Mylon, S. E.; Ferri, J. Programming Nanoparticle Aggregation Kinetics with Poly(MeO2MA-*co*-OEGMA) CoPolymers. *Soft Matter* **2013**, *9*, 11046−11053.
(46) Edwards, E. W.; Chanana, M.; Wang, D. Capping Gold Nanoparticles with Stimuli-responsive Polymers to Cross Water−Oil Interfaces: In-Depth Insight to the Trans-Interfacial Activity of Nanoparticles. *J. Phys. Chem. C* **2008**, *112*, 15207−15219.
(47) Chanana, M.; Jahn, S.; Georgieva, R.; Lutz, J.-F.; Bäumler, H.; Wang, D. Fabrication of Colloidal Stable, Thermosensitive, and Biocompatible Magnetite Nanoparticles and Study of Their Reversible Agglomeration in Aqueous Milieu. *Chem. Mater.* **2009**, *21*, 1906−1914.
(48) Gambinossi, F.; Lapides, D.; Anderson, C.; Chanana, M.; Ferri, J. K. Effect of Nanoparticle Surface Chemistry on Adsorption and Fluid Partitioning in Aqueous/Toluene and Cellular Systems. *J. Nanosci. Nanotechnol.* **2014**, *15*, 3610−3617.
(49) Sefcik, L.; Kaminski, A.; Ling, K.; Laschewsky, A.; Lutz, J.-F.; Wischerhoff, E. Effects of PEG-Based Thermoresponsive Polymer Brushes on Fibroblast Spreading and Gene Expression. *Cell. Mol. Bioeng.* **2013**, *6*, 287−298.
(50) Houben, J.; Müller, E.; Büchel, K. H.; Padeken, H. G. *Methods of Organic Chemistry (Houben-Weyl);* G. Thieme: Stuttgart, Germany, 1995.
(51) Zeppieri, S.; Rodríguez, J.; López de Ramos, A. L. Interfacial Tension of Alkane + Water Systems. *J. Chem. Eng. Data* **2001**, *46*, 1086−1088.
(52) Wischerhoff, E.; Glatzel, S.; Uhlig, K.; Lankenau, A.; Lutz, J.-F.; Laschewsky, A. Tuning the Thickness of Polymer Brushes Grafted from Nonlinearly Growing Multilayer Assemblies. *Langmuir* **2009**, *25*, 5949−5956.
(53) Uhlig, K.; Boysen, B.; Lankenau, A.; Jaeger, M.; Wischerhoff, E.; Lutz, J.-F.; Laschewsky, A.; Duschl, C. On the Influence of the Architecture of Poly(ethylene glycol)-based Thermoresponsive Polymers on Cell Adhesion. *Biomicrofluidics* **2012**, *6*, 024129.
(54) Kwok, D. Y.; Lin, R.; Mui, M.; Neumann, A. W. Low-rate Dynamic and Static Contact Angles and the Determination of Solid Surface Tensions. *Colloids Surf., A* **1996**, *116*, 63−77.
(55) Rotenberg, Y.; Boruvka, L.; Neumann, A. W. Determination of Surface Tension and Contact Angle from the Shapes of Axisymmetric Fluid Interfaces. *J. Colloid Interface Sci.* **1983**, *93*, 169−183.
(56) Neumann, A. W.; David, R.; Zuo, Y. *Applied Surface Thermodynamics,* 2nd ed.; Taylor & Francis: Milton Park, Abingdon, U.K., 2011.
(57) Horcas, I.; Fernandez, R.; Gomez-Rodriguez, J. M.; Colchero, J.; Gomez-Herrero, J.; Baro, A. M. WSXM: A Software for Scanning Probe Microscopy and a Tool for Nanotechnology. *Rev. Sci. Instrum.* **2007**, *78*, 013705−8.
(58) Wenzel, R. N. Surface Roughness and Contact Angle. *J. Phys. Colloid Chem.* **1949**, *53*, 1466−1467.
(59) Ferri, J. K.; Dong, W.-F.; Miller, R. Ultrathin Free-Standing Polyelectrolyte Nanocomposites: A Novel Method for Preparation and Characterization of Assembly Dynamics. *J. Phys. Chem. B* **2005**, *109*, 14764−14768.
(60) Lutz, J.-F.; Hoth, A. Preparation of Ideal PEG Analogues with a Tunable Thermosensitivity by Controlled Radical Copolymerization of 2-(2-Methoxyethoxy)ethyl Methacrylate and Oligo(ethylene glycol) Methacrylate. *Macromolecules* **2005**, *39*, 893−896.
(61) Zhulina, E. B.; Borisov, O. V.; Pryamitsyn, V. A.; Birshtein, T. M. Coil-Globule Type Transitions in Polymers. 1. Collapse of Layers of Grafted Polymer Chains. *Macromolecules* **1991**, *24*, 140−149.
(62) Zengin, A.; Yildirim, E.; Caykara, T. RAFT-Mediated Synthesis and Temperature-Induced Responsive Properties of Poly(2-(2-methoxyethoxy)ethyl methacrylate) Brushes. *J. Polym. Sci., Part A: Polym. Chem.* **2013**, *51*, 954−962.

DOI: 10.1021/am507418m
ACS Appl. Mater. Interfaces 2015, 7, 2518−2528

(63) Quéré, D. Wetting and Roughness. *Annu. Rev. Mater. Res.* **2008**, *38*, 71−99.
(64) Dey, S.; Kellam, B.; Alexander, M. R.; Alexander, C.; Rose, F. R. A. J. Enzyme-Passage Free Culture of Mouse Embryonic Stem Cells on Thermo-Responsive Polymer Surfaces. *J. Mater. Chem.* **2011**, *21*, 6883−6890.
(65) Cassie, A. B. D.; Baxter, S. Wettability of Porous Surfaces. *Trans. Faraday Soc.* **1944**, *40*, 546−551.
(66) Ishizu, K.; Sawada, N.; Satoh, J.; Sogabe, A. Architecture and Surfactant Behavior of Amphiphilic Prototype Copolymer Brushes. *J. Mater. Sci. Lett.* **2003**, *22*, 1219−1222.
(67) Adamson, A. W. *Physical Chemistry of Surfaces;* Wiley: Hoboken, NJ, 1990.
(68) Li, D.; Neumann, A. W. A Reformulation of the Equation of State for Interfacial Tensions. *J. Colloid Interface Sci.* **1990**, *137*, 304−307.
(69) Li, D.; Neumann, A. W. Contact Angles on Hydrophobic Solid Surfaces and their Interpretation. *J. Colloid Interface Sci.* **1992**, *148*, 190−200.
(70) Joy, A.; Cohen, D. M.; Luk, A.; Anim-Danso, E.; Chen, C.; Kohn, J. Control of Surface Chemistry, Substrate Stiffness, and Cell Function in a Novel Terpolymer Methacrylate Library. *Langmuir* **2011**, *27*, 1891−1899.

DOI: 10.1021/am507418m
ACS Appl. Mater. Interfaces 2015, 7, 2518−2528